(15) Fajans, K. *Chem. Ber.* **1920**, *53*, 643.
(16) (a) Wiener, H. *J. Am. Chem. Soc.* **1947**, *69*, 17. (b) Wiener, H. *J. Am. Chem. Soc.* **1947**, *69*, 2636. (c) Wiener, H. *J. Phys. Chem.* **1948**, *52*, 425. (d) Wiener, H. *J. Phys. Chem.* **1948**, *52*, 1082.
(17) (a) Platt, J. R. *J. Chem. Phys.* **1947**, *15*, 419. (b) Platt, J. R. *J. Phys. Chem.* **1952**, *56*, 328.
(18) Franklin, J. F. *Ind. Eng. Chem.* **1949**, *41*, 1070.
(19) Laidler, K. J. *Can. J. Chem.* **1956**, *34*, 626.
(20) Benson, S. W.; Buss, J. H. *J. Chem. Phys.* **1958**, *29*, 546.
(21) Allen, T. L. *J. Chem. Phys.* **1959**, *31*, 1039.
(22) Skinner, H. A. *J. Chem. Soc.* **1962**, 4396.
(23) Skinner, H. A.; Pilcher, G. *Q. Rev. Chem. Soc.* **1963**, *17*, 264.
(24) Gordon, M.; Scatlebury, G. R. *Trans. Faraday Soc.* **1964**, *60*, 604.
(25) Smolenskii, E. E. *Zh. Fiz. Khim.* **1964**, *38*, 1288.
(26) Kalb, A. J.; Chung, A. L. H.; Allen, T. L. *J. Am. Chem. Soc.* **1966**, *88*, 13.
(27) Benson, S. W.; Cruickshank, F. R.; Golden, D. M.; Haugen, G. R.; O'Neal, H. E.; Rodgers, A. S.; Shaw, R.; Walsh, R. *Chem. Rev.* **1969**, *69*, 279.
(28) Good, W. D. *J. Chem. Eng. Data* **1969**, *14*, 231.
(29) Hosoya, H. *Bull. Chem. Soc. Jpn.* **1971**, *44*, 2332.
(30) (a) Somayajulu, G. R.; Zwolinski, B. J. *J. Chem. Soc., Faraday Trans. 2* **1972**, *68*, 1971. (b) *Ibid.* **1974**, *70*, 967. (c) *Ibid.* **1974**, *70*, 973.
(31) Gordon, M.; Kennedy, J. W. *J. Chem. Soc., Faraday Trans. 2* **1973**, *69*, 484.
(32) Kao, J. W. H.; Chung-Phillips, A. *J. Chem. Phys.* **1975**, *63*, 4143.
(33) Gasteiger, J.; Jacob, P.; Strauss, U. *Tetrahedron* **1979**, *35*, 139.
(34) (a) Edward, J. T. *Can. J. Chem.* **1980**, *58*, 1897. (b) *Ibid.* **1981**, *59*, 3192.
(35) Guthrie, J. P.; Taylor, K. F. *Can. J. Chem.* **1984**, *62*, 363.
(36) Needham, D. E.; Wei, I.-C.; Seybold, P. G. *J. Am. Chem. Soc.* **1988**, *110*, 4186.
(37) McHughes, M. C.; Poshuta, R. D. *J. Math. Chem.* **1990**, *4*, 227.
(38) Cox, J. D.; Pilcher, G. *Thermochemistry of Organic and Organometallic Compounds*; Academic Press: New York, 1970.
(39) Pedley, J. B.; Naylor, R. D.; Kirby, S. P. *Thermochemical Data of Organic Compounds*, 2nd ed., Chapman and Hall: New York, 1986.
(40) Bendel, R. B.; Afifi, A. A. *J. Am. Stat. Assoc.* **1977**, *72*, 46.
(41) Radhakrishnan, T. P.; Herndon, W. C. *J. Math. Chem.* **1988**, *2*, 391. Also see ref 34.

Applications of Graph Theory and Topology for the Study of Aromaticity in Inorganic Compounds[1]

R. B. KING

Department of Chemistry, University of Georgia, Athens, Georgia 30602

Received August 27, 1991

The topology of overlap of the atomic orbitals participating in the requisite delocalization for an aromatic system can be described by a graph, the eigenvalue spectrum of which can be related to molecular orbital energy parameters as determined by Hückel theory. Such aromatic systems can be classified according to the nodality of the overlapping atomic orbitals. Thus, the three-dimensional deltahedral boranes $B_nH_n^{2-}$ and carboranes $B_{n-2}C_2H_n$ ($6 \le n \le 12$) are examples of anodal orbital aromatic systems since the delocalization in their bonding arises from overlap of anodal radial boron or carbon sp hybrids. Two-dimensional planar polygonal hydrocarbons such as cyclopentadienide, benzene, and tropylium are examples of uninodal orbital aromatic systems since the delocalization in their bonding arises from overlap of uninodal *p* orbitals at each of the carbon vertices. Similarly, three-dimensional polyoxometallates such as octahedral $M_6O_{19}^{n-}$ and cuboctahedral $XM_{12}O_{40}^{n-}$ are examples of binodal orbital aromatic systems since the delocalization in their bonding arises from overlap of the binodal d_{xy} orbitals at each of the metal vertices. The delocalization in these binodal aromatic systems is much weaker than that in the uninodal and anodal aromatic systems since the relevant orbital overlap in the binodal aromatic systems must occur through indirect M–O–M bonds rather than direct vertex–vertex bonds.

INTRODUCTION

Important ideas arising from molecular orbital theory[2-4] include the concepts of resonance energy and aromaticity. Graph-theory derived methods have subsequently been used to refine these ideas,[5-7] which were initially applied to two-dimensional planar hydrocarbons [e.g., cyclopentadienide ($C_5H_5^-$), benzene (C_6H_6), and tropylium ($C_7H_7^+$)] and corresponding heterocycles [e.g., pyridine (C_5H_5N) and thiophene (C_4H_4S)]. More recently the concepts of resonance energy and aromaticity have been extended to the three-dimensional deltahedral boranes $B_nH_n^{2-}$ and carboranes $C_2B_{n-2}H_n$ ($6 \le n \le 12$) in which the boron and/or carbon atoms form the deltahedra depicted in Figure 1. In this context a *deltahedron* is defined as a polyhedron in which all faces are triangles like the Greek letter *delta*, Δ. The Wade analogy[8-11] [e.g., between $Fe(CO)_3$ and BH vertices or $Co(CO)_3$ and CH vertices] makes similar ideas applicable to transition-metal clusters consisting of metal deltahedra [e.g., the octahedral $Rh_6(CO)_{16}$ or the icosahedral[12] $Ni_{12}E(CO)_{22}^{2-}$ where E = Ge, Sn]. Related ideas recently[13] have been shown to be applicable to electron delocalization in the readily reducible early-transition-metal polyoxometallates, which may be regarded as three-dimensional aromatic systems based on a large octahedron or cuboctahedron (Figure 2) of transition-metal atoms.

Previous considerations of aromaticity in polygonal or polyhedral clusters have focused on the dimensionality of the structure.[14] Thus the planar polygonal hydrocarbons $C_5H_5^-$, C_6H_6, and $C_7H_7^+$ are two-dimensional aromatic systems whereas the deltahedral boranes ($B_nH_n^{2-}$) and carboranes ($C_2B_{n-2}H_n$) as well as the polyoxometalates are three-dimensional aromatic systems. This paper focuses on another aspect of the aromaticity in these systems, namely, the nodality of the valence orbitals of the vertex atoms participating in the delocalization. An outline of the graph-theoretical approach to aromaticity is first presented.

BACKGROUND

A graph *G* is defined[15] as a finite nonempty set *V* (the *vertices*) together with a (possibly empty) set *E* (the *edges*—disjoint from *V*) of two-element subsets of (distinct) elements of *V*. In the graph-theoretical bonding models discussed in this paper, the set *V* or vertices represent skeletal atoms or

0095-2338/92/1632-0042$03.00/0

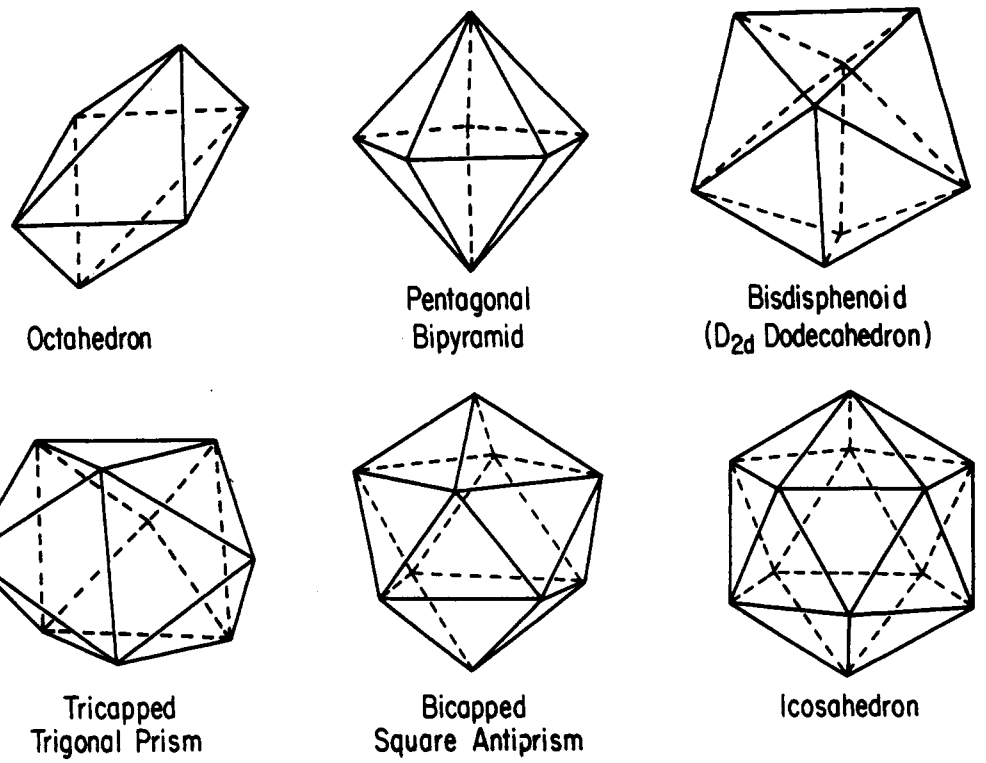

Figure 1. Deltahedra found in the borane anions $B_nH_n^{2-}$ and carboranes $B_{n-2}C_2H_n$.

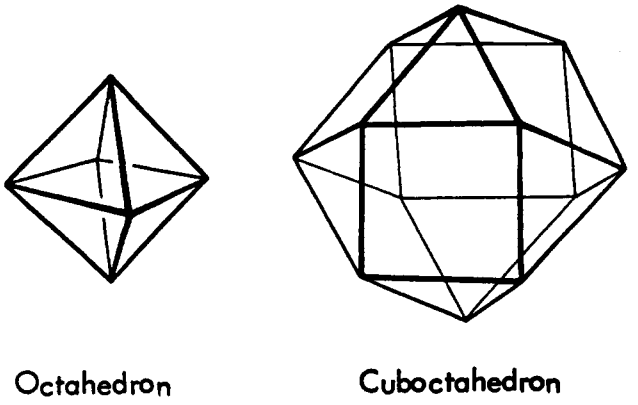

Figure 2. Regular octahedron and cuboctahedron.

more precisely their valence orbitals, and the set E or edges represent bonding relationships between pairs of skeletal atoms. The graph G representing bonding relationships in a delocalized polyhedral molecule will *not* correspond to the 1-skeleton[16] consisting of the edges of the polyhedron since the bonding relationships are not localized along the edges of the polyhedron.

Ideas based on graph theory can be used to describe Hückel theory, which was first applied to conventional two-dimensional aromatic systems.[17-20] The graph G is used to describe the overlap of the atomic orbitals involved in the delocalized bonding in aromatic systems in which the vertices V correspond to orbitals and the edges E correspond to orbital overlaps. The adjacency matrix[21] **A** of such a graph can be defined as follows:

$$A_{ij} = \begin{cases} 0 \text{ if } i = j \\ 1 \text{ if } i \text{ and } j \text{ are connected by an edge} \\ 0 \text{ if } i \text{ and } j \text{ are not connected by an edge} \end{cases} \quad (1)$$

The eigenvalues of the adjacency matrix are obtained from the following determinantal equation:

$$|\mathbf{A} - x\mathbf{I}| = 0 \quad (2)$$

in which **I** is the unit matrix ($I_{ii} = 1$ and $I_{ij} = 0$ for $i \neq j$). These topologically derived eigenvalues are closely related to the energy levels as determined by Hückel theory which uses the secular equation

$$|\mathbf{H} - E\mathbf{S}| = 0 \quad (3)$$

Note the general similarities between eqs 2 and 3. In eq 3 the energy matrix **H** and the overlap matrix **S** can be resolved into the identity matrix **I** and the adjacency matrix **A** as follows:

$$\mathbf{H} = \alpha\mathbf{I} + \beta\mathbf{A} \quad (4)$$

$$\mathbf{S} = \mathbf{I} + S\mathbf{A}$$

The energy levels of the Hückel molecular orbitals (eq 3) are thus related to the eigenvalues x_k of the adjacency matrix **A** (eq 2) by the following equation:

$$E_k = \frac{\alpha + x_k\beta}{1 + x_kS} \quad (5)$$

In eq 5, α is the standard Coulomb integral, assumed to be the same for all atoms, β is the resonance integral taken to be the same for all bonds, and S is the overlap integral between atomic orbitals on neighboring atoms.

The two extreme types of skeletal chemical bonding in polygonal or polyhedral molecules may be called *edge-localized* and *globally delocalized*.[22-25] An edge-localized polygon or polyhedron has two-electron two-center bonds along each edge and is favored when the number of internal orbitals from each vertex atom matches the degree of the corresponding vertex. A globally delocalized polygon or polyhedron has a multicenter bond involving all of the vertex atoms; such global delocalization is a feature of fully aromatic systems. Delocalization is favored when the numbers of internal orbitals do *not* match the vertex degrees.

The graph-theoretical model of aromaticity uses a graph G to describe the overlap of valence orbitals represented by its vertices V. Such valence orbitals can be classified by their *nodalities*, i.e., the number of nodal planes. Thus an *anodal* orbital has no nodal planes like an s orbital and is the type of hybrid orbital used in σ-bonding. A *uninodal* orbital has

Table I. Types of Aromaticity

compd type	formulas	dimensionality	vertex atoms	overlapping orbitals: type	overlapping orbitals: nodes	adjacent atom interactions	structure
deltahedral borane anions	$B_nH_n^{2-}$ ($6 \le n \le 12$)	3	B	sp	0	B–B	I
planar hydrocarbons	$C_nH_n^{6-n}$	2	C	p	1	C–C	II
macrooctahedral and macrocuboctahedral polyoxometalates	$M_6O_{19}^{m-}$ $XM_{12}O_{40}^{n-}$ (M = V, Nb, Mo, W)	3	M	d	2	M–O–M	III

a single nodal plane like a p orbital, and a *binodal* orbital has two nodal planes like a d orbital. The types of aromaticity arising from this classification are given in Table I.

The deltahedral boranes are examples of aromatic systems constructed from anodal orbitals. The vertex B–H unit in a deltahedral borane anion $B_nH_n^{2-}$ can be depicted as follows:

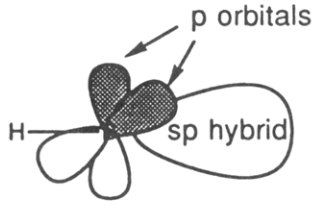

I

In structure **I** the boron atom has two anodal sp hybrids. The sp hybrid depicted by a balloon participates in the delocalized bonding represented by the graph *G*. The deltahedral boranes are thus anodal orbital aromatic systems. The planar polygonal hydrocarbons are examples of aromatic systems constructed from uninodal orbitals. The vertex C–H unit in $C_5H_5^-$, C_6H_6, or $C_7H_7^+$ can be depicted as follows:

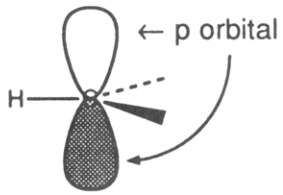

II

In structure **II** the uninodal p orbital of the carbon atom participates in the delocalized bonding represented by the graph *G*. The planar polygonal hydrocarbons are thus uninodal orbital aromatic systems. In an analogous way the polyoxometallates may be considered to be examples of aromatic systems constructed from binodal orbitals. Such polyoxometallates can be constructed from $(\mu_n\text{-O})_5MO$ vertices where μ_n-O refers to either doubly-bridging (μ_2-O) or triply-bridging (μ_3-O) oxygen atoms, and O refers to a single multiply-bonded terminal oxygen atom on each metal atom. These vertex $(\mu_n\text{-O})_5MO$ units can be depicted as follows:

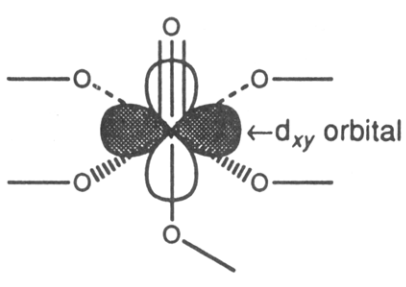

III

In structure **III** one of the five d valence orbitals of the central transition-metal atom cannot participate in any of the metal–oxygen bonding and thus is available to overlap with the analogous d orbitals of adjacent $(\mu_n\text{-O})_5MO$ units to form a delocalized system. These three general types of aromatic systems, classified according to the nodality of the orbitals involved in the delocalization, will be discussed in greater detail in the next section. The two-dimensional uninodal aromatic systems will be treated first since they are the least complicated.

AROMATIC SYSTEMS

Uninodal Orbital Aromatic Systems. The graph-theoretical approach to aromaticity is best illustrated by first considering benzene as a prototypical planar polygonal aromatic hydrocarbon since other approaches to the bonding in benzene are familiar to many chemists. A CH vertex of benzene can be represented schematically by structure **II**, depicted in the previous section. The four carbon valence orbitals of the sp^3 manifold are divided into three sp^2 hybrids and a single p orbital. One of the sp^2 hybrids is bonded to the external hydrogen atom leaving two sp^2 hybrids and the p orbital as internal orbitals. Among the three internal orbitals the two equivalent sp^2 hybrids are twin internal orbitals or *tangential* orbitals whereas the single p orbital is a unique internal orbital or *radial* orbital. The uninodality of this unique internal orbital defines the nodality of the aromaticity.

The internal orbitals of the six carbon atoms form the benzene skeletal bonding including the delocalization responsible for its aromaticity. Pairwise overlap of the (2)(6) = 12 twin internal orbitals around the circumference of the hexagon is responsible for splitting these 12 orbitals into 6 σ-bonding and 6 σ^*-antibonding orbitals leading to the so-called σ-bonding of benzene. This localized bonding has a dimensionality of one, i.e., one less than the dimensionality of two of this aromatic system.

The σ-bonding of benzene is supplemented by the so-called π-bonding arising from overlap of the six unique internal orbitals, namely the single p orbital on each of the carbon atoms (see structure **II**). The overlap of these unique internal orbitals can be described by the C_6 cyclic graph, which is the hexagon. The eigenvalue spectrum of the hexagon (eq 2) is +2, +1, +1, −1, −1, −2 (Figure 3, lower right) leading to three π-bonding and three π^*-antibonding orbitals. The total benzene skeleton thus has nine bonding orbitals (6σ and 3π) which are filled by the 18 skeletal electrons which arise when each of the CH vertices contributes three skeletal electrons. Twelve of these skeletal electrons are used for the σ-bonding and the remaining six electrons for the π-bonding.

Figure 3 also illustrates how the delocalized bonding in benzene from the C_6 overlap of the unique internal orbitals, namely, the p orbitals, leads to aromatic stabilization. In a hypothetical localized "cyclohexatriene" structure where the interactions between the p orbitals on each carbon atom are pairwise interactions, the corresponding graph *G* (Figure 3, upper left) consists of three disconnected line segments (i.e., $3 \times K_2$). This graph has three +1 eigenvalues and three −1 eigenvalues. Filling each of the corresponding three bonding orbitals with an electron pair leads to an energy of 6β from this π-bonding. In a delocalized "benzene" structure where the delocalized interactions between the p orbitals on each carbon atom are described by the cyclic C_6 graph (Figure 3,

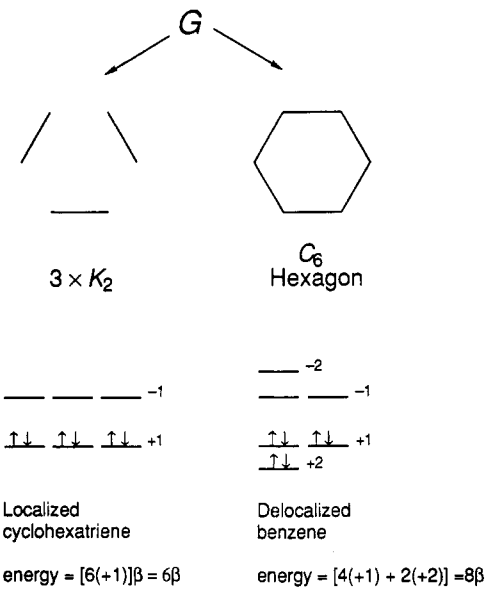

Figure 3. Molecular orbital energy parameters determined by graph spectra and aromatic delocalization energies in benzene showing the graphs G corresponding to the $3 \times K_2$ "cyclohexatriene" and the C_6 hexagon "benzene".

upper right), filling the three bonding orbitals with an electron pair each leads to an energy of 8β. This corresponds to a resonance stabilization of $8\beta - 6\beta = 2\beta$ arising from the delocalized bonding of the carbon p orbitals in benzene. We will see below how similar ideas can be used to describe the three-dimensional aromaticity in deltahedral boranes.

Anodal Orbital Aromatic Systems. The anodal aromatic systems are exemplified by the deltahedral boranes $B_nH_n^{2-}$ and carboranes $B_{n-2}C_2H_n^{2-}$ ($6 \leq n \leq 12$) based on deltahedra (Figure 1), with vertices of degrees four and five being strongly favored. Consider the simplest deltahedral borane, namely, the octahedral $B_6H_6^{2-}$, as an example of such a deltahedral borane. A BH vertex of $B_6H_6^{2-}$ can be represented schematically by structure I, depicted in the previous section. The four boron valence orbitals of its sp^3 manifold are divided into two sp hybrids and two extra p orbitals. One of the sp hybrids is bonded to an external hydrogen atom leaving the second sp hybrid and the two extra p orbitals as internal orbitals. Among these three internal orbitals, the two equivalent p orbitals are the twin internal orbitals or *tangential* orbitals whereas the single sp hybrid is a unique internal orbital or *radial* orbital. The anodality of this unique internal orbital defines the anodality of this aromaticity.

The internal orbitals of the six boron atoms form the skeletal bonding in $B_6H_6^{2-}$ including the delocalization responsible for its aromaticity. The pairwise overlap of the $(2)(6) = 12$ twin internal orbitals, namely, the two p orbitals on each of the six boron atoms, leads to six bonding and six antibonding orbitals over the surface of the polyhedron. This *surface* bonding has a dimensionality of two, namely, one dimension less than the three-dimensional deltahedron. In addition, this surface bonding may be regarded as the three-dimensional analogue of the σ-bonding in benzene.

The surface bonding in $B_6H_6^{2-}$ is supplemented by *core* bonding arising from overlap of the six unique internal orbitals, which are the single sp hybrids on each of the six boron atoms directed toward the core of the polyhedron. The topology of this core bonding can be represented by a graph G_c. The two limiting possibilities for G_c for a deltahedral borane or carborane are the complete graph K_n and the deltahedral graph D_n, and the corresponding core-bonding topologies may be called the *complete* and *deltahedral* topologies, respectively. In the complete graph K_n, each vertex has an edge going to every other vertex, leading to a total of $n(n-1)/2$ edges.[26] For any value of n, the complete graph K_n has only one positive eigenvalue, namely, $n - 1$, and $n - 1$ negative eigenvalues, namely, -1 each. The deltahedral graph D_n is identical to the 1-skeleton of the deltahedron. Thus, two vertices of D_n are connected by an edge if, and only if, the corresponding vertices of the deltahedron are connected by an edge. The graph D_n for the deltahedra of interest with seven or more vertices all have at least three positive eigenvalues but one of these eigenvalues, conveniently called the *principal eigenvalue*, is much more positive than any other of the positive eigenvalues. The bonding molecular orbital from the delocalized core bonding in a deltahedral borane or carborane corresponding to the single positive eigenvalue of K_n or the principal eigenvalue of D_n may be called the *principal* core orbital. Since deltahedral boranes $B_nH_n^{2-}$ and carboranes $B_{n-2}C_2H_n$ have $2n + 2$ skeletal electrons, of which $2n$ are used for the surface bonding, there are only two electrons available for the core bonding, corresponding to a single core-bonding molecular orbital and a single positive eigenvalue for G_c. Thus, deltahedral boranes are three-dimensional aromatic systems with $4k + 2 = 2$ core-bonding electrons where $k = 0$, analogous to the $4k + 2$ π-electrons where $k = 0$ ($C_3H_3^+$), 1 ($C_5H_5^-$, C_6H_6, $C_7H_7^+$), or 2 ($C_8H_8^{2-}$) for the planar two-dimensional uninodal orbital aromatic systems discussed above. Furthermore, only if G_c is taken to be the corresponding complete graph K_n will the simple model given above for globally delocalized deltahedra give the correct number of skeletal electrons in all cases, namely $2n + 2$ skeletal electrons for $6 \leq n \leq 12$. Such a model with complete core-bonding topology is the basis for the graph-theory-derived model for the chemical-bonding topology of deltahedral boranes and carboranes discussed in previous papers. However, the deltahedral core-bonding topology represented by the deltahedral graph D_n can also account for the observed $2n + 2$ skeletal electrons in the $B_nH_n^{2-}$ deltahedral boranes if there is a mechanism for raising the energies of all of the core molecular orbitals other than the principal core orbital to antibonding energy levels. This possibility was already indicated in the original graph-theoretical analysis[27] of the $3n$ Hoffmann–Lipscomb LCAO–MO extended Hückel computations[28] on icosahedral $B_{12}H_{12}^{2-}$, which showed that the four core orbitals corresponding to positive eigenvalues of the icosahedral graph D_{12} would be bonding orbitals except for core-surface orbital mixing, which raises the energies of three of these four core orbitals to antibonding levels, leaving only the principal core orbital as a bonding-core orbital.

Figure 4 illustrates how the delocalized bonding in $B_6H_6^{2-}$ arising from overlap of the unique internal orbitals, namely, the radial sp hybrids on each boron atom, can lead to aromatic stabilization. In a hypothetical localized structure where the interactions between the radial sp hybrids are pairwise interactions, the corresponding graph G_c (Figure 4, left) is three disconnected line segments (i.e., $3 \times K_2$). The spectrum of this graph has three $+1$ eigenvalues and three -1 eigenvalues. Filling one of the bonding orbitals with the available two core-bonding electrons leads to an energy of 2β from the core bonding. In a completely delocalized structure where the core bonding is described by the complete graph K_6 (Figure 4, right), this electron pair is in a bonding orbital with an eigenvalue of $+5$ corresponding to an energy of $(2)(5\beta) = 10\beta$. The aromatic stabilization of completely delocalized $B_6H_6^{2-}$ is thus $10\beta - 2\beta = 8\beta$ assuming the same β unit for both the localized and complete delocalized structures. In an octahedrally delocalized $B_6H_6^{2-}$ where the core bonding is described by the deltahedral graph D_6 corresponding to the 1-skeleton of the octahedron (Figure 4, center), the core-bonding electron pair is in a bonding orbital with an eigenvalue of $+4$ corresponding to an energy of $(2)(4\beta) = 8\beta$. The aromatic sta-

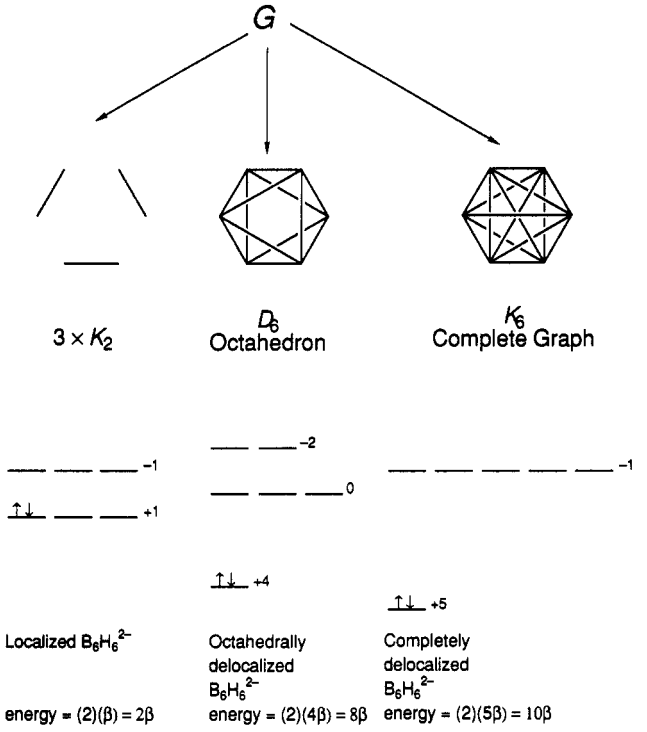

Figure 4. Molecular orbital energy parameters determined by graph spectra and aromatic delocalization energies in $B_6H_6^{2-}$ showing the graphs G corresponding to the $3 \times K_2$ localized structure, the D_6 octahedrally delocalized, and the K_6 completely delocalized structure.

bilization of octahedrally delocalized $B_6H_6^{2-}$ is thus $8\beta - 2\beta = 6\beta$. Thus the aromatic stabilization of $B_6H_6^{2-}$ is considerable regardless of whether the delocalized core bonding is considered to have the complete topology represented by the complete graph K_6 or the octahedral topology represented by the deltahedral graph D_6.

Binodal Orbital Aromatic Systems. Heteropoly- and isopolyoxometallates of early transition metals[29,30] constructed from MO_6 octahedra with only one terminal oxygen atom may be regarded as examples of binodal orbital aromatic systems. An MO_6 vertex [or more precisely a $(\mu_n\text{-O})_5MO$ vertex] building block for such structures is depicted in structure **III** in the previous section. In such an $(\mu_n\text{-O})_5MO$ vertex only eight of the nine orbitals of the sp^3d^5 manifold of M can be used for the σ- and π-bonding to the single terminal oxygen atom and the σ-bonding to the five bridging oxygen atoms leaving one nonbonding d orbital [d_{xy} if the M≡O(terminal) axis is the z-axis]. This d_{xy} orbital may be regarded as a unique internal orbital. Thus a $(\mu_n\text{-O})_5MO$ vertex with a nominally nonbonding d_{xy} valence orbital in a polyoxometallate (structure **III**) is analogous to an unsaturated CH vertex with a nonbonding p orbital in a planar aromatic hydrocarbon such as benzene (structure **II**). The binodality of the nonbonding d_{xy} orbital of a $(\mu_n\text{-O})_5MO$ vertex defines the binodality of the aromaticity in the polyoxometallates.

The networks formed by the $(\mu_n\text{-O})_5MO$ vertices in the polyoxometallates can be described by the large polyhedron formed by the metal atoms M as vertices. In general the edges of this *macropolyhedron* are M–O–M bridges, and with rare exceptions there is no direct metal–metal bonding. Since the polyoxometallates are constructed from macropolyhedra having relatively long M–O–M edges rather than normal metal polyhedra with much shorter M–M edges, the direct overlap of the d_{xy} orbitals on different metal atoms is negligible. Instead the metal–metal interactions using these metal d_{xy} orbitals must also involve the orbitals of the oxygen atoms in the M–O–M bridges[31] and thus resemble the exchange coupling between metal atoms in antiferromagnetic systems.[32]

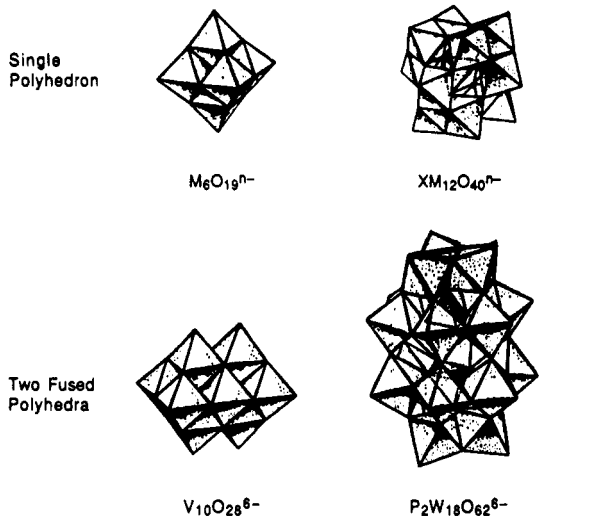

Figure 5. Structures of aromatic polyoxometallates based on metal macrooctahedra (left) and metal macrocuboctahedra (right).

Thus the electron delocalization in polyoxometallates with $(\mu_n\text{-O})_5MO$ vertices is based on indirect M–O–M interactions using the metal d_{xy} and appropriate bridging oxygen p orbitals rather than direct M–M interactions such as those found in metal clusters. For this reason electron delocalization in the binodal orbital aromatic polyoxometallates is much weaker than that in either the uninodal aromatic planar aromatic hydrocarbons or the anodal orbital aromatic three-dimensional deltahedral boranes and carboranes discussed above. This weaker interaction translates to a much lower value of the parameter β in eq 5.

The improper 4-fold symmetry (S_4) of the nonbonding d_{xy} orbitals in the $(\mu_n\text{-O})_5MO$ vertices of the polyoxometallates has an important effect on the favored macropolyhedra for their structures. Matching this improper 4-fold orbital symmetry with the overall macropolyhedral symmetry requires macropolyhedra in which a C_4 axis passes through each vertex. A true three-dimensional polyhedron having C_4 axes passing through each vertex can have only O or O_h symmetry (the only point groups having multiple C_4 axes). The only polyhedra with less than 15 vertices meeting these highly restrictive conditions are the regular octahedron and the cuboctahedron (Figure 2). It is therefore not surprising that these two polyhedra form the basis of the specific early transition-metal polyoxometallate structures containing only $(\mu_n\text{-O})_5MO$ vertices. These structures are illustrated in Figure 5.

Consider the octahedral and cuboctahedral topologies of the indirect overlap of the d_{xy} orbitals in derivatives such as the octahedral polyoxometallates $M_6O_{19}^{n-}$ and the cuboctahedral polyoxometallates $XM_{12}O_{40}^{n-}$, respectively. The octahedron has the eigenvalues +4, 0, and −2 with degeneracies 1, 3, and 2, respectively (Figure 4, center), whereas the cuboctahedron has the eigenvalues +4, +2, 0, and −2 with degeneracies 1, 3, 3, and 5, respectively. The most positive eigenvalue of +4 for both polyhedra arises from the fact that each polyhedron corresponds to a regular graph of valence 4.[33] This highly positive principal eigenvalue corresponds to a highly bonding molecular orbital which can accommodate the first two electrons upon reduction of the initially d^0 polyoxometallates of the types $M_6O_{19}^{n-}$ and $XM_{12}O_{40}^{n-}$. The reported[34,35] diamagnetism of the two-electron reduction products of the $PW_{12}O_{40}^{3-}$, $SiW_{12}O_{40}^{4-}$, and $[(H_2)W_{12}O_{40}]^{6-}$ anions is in accord with the two electrons being paired in this lowest lying molecular orbital. Thus the overlap of the otherwise nonbonding d_{xy} orbitals in the $M_6O_{19}^{n-}$ and $XM_{12}O_{40}^{n-}$ d^0 early-transition-metal polyoxometallates creates a low-lying bonding molecular orbital which can accommodate two electrons,

thereby facilitating reduction of polyoxometallates of these types.

The concept of binodal orbital aromaticity in reduced early-transition-metal polyoxometallates may be related to their classification as mixed valence compounds. Robin and Day[36] classify mixed valence compounds into the following three classes: Class I, fully localized corresponding to an insulator in an infinite system; Class II, partially delocalized corresponding to a semiconductor in an infinite system; and Class III, completely delocalized corresponding to a metal in an infinite system. ESR studies on the one-electron reduced polyoxometallates $M_6O_{19}^{n-}$ and $XM_{12}O_{40}^{n-}$ suggest class II mixed valence species.[37,38] Although such species are delocalized at accessible temperatures, they behave as localized systems at sufficiently low temperatures similar to semiconductors. This is in accord with the much smaller overlap (i.e., lower β in eq 5) of the metal d_{xy} orbitals associated with binodal orbital aromaticity as compared with the boron sp hybrid anodal internal orbitals in the deltahedral boranes $B_nH_n^{2-}$ or the carbon uninodal p orbitals in benzene.

REFERENCES AND NOTES

(1) Paper presented to the American Chemical Society Division of Computers in Chemistry at the Symposium on *Chemical Applications of Graph Theory* in conjunction with the Fourth Chemical Congress of North America, New York, Aug 1991.
(2) Streitwieser, A., Jr. *Molecular Orbital Theory for Organic Chemists*; Wiley: New York, 1961.
(3) Salem, L. *The Molecular Orbital Theory of Conjugated Systems*; Benjamin: New York, 1966.
(4) Dewar, M. J. S. *The Molecular Orbital Theory of Organic Chemistry*; McGraw-Hill: New York, 1969.
(5) Aihara, J. *Bull. Chem. Soc. Jpn.* **1975**, *48*, 517.
(6) Aihara, J. *Bull. Chem. Soc. Jpn.* **1975**, *48*, 1501.
(7) Aihara, J. *J. Am. Chem. Soc.* **1976**, *98*, 2750.
(8) Wade, K. *Chem. Commun.* **1971**, 792.
(9) Mingos, D. M. P. *Nature (London), Phys. Sci.* **1972**, *236*, 99.
(10) Wade, K. *Adv. Inorg. Chem. Radiochem.* **1976**, *18*, 1.
(11) Mingos, D. M. P. *Acc. Chem. Res.* **1984**, *17*, 311.
(12) Ceriotti, A.; Demartin, F.; Heaton, B. T.; Ingallina, P.; Longoni, G.; Manassero, M.; Marchionna, M.; Masciocchi, N. *Chem. Commun.* **1989**, 786.
(13) King, R. B. *Inorg. Chem.* **1991**, *30*, 4437.
(14) King, R. B. *J. Math. Chem.* **1987**, *1*, 249.
(15) Behzad, M.; Chartrand, G. *Introduction to the Theory of Graphs*; Allyn and Bacon: Boston, 1971; section 1.1.
(16) Grünbaum, B. *Convex Polytopes*; Interscience: New York, 1967.
(17) Ruedenberg, K. *J. Chem. Phys.* **1954**, *22*, 1878.
(18) Schmidtke, H. H. *J. Chem. Phys.* **1966**, *45*, 3920.
(19) Schmidtke, H. H. *Coord. Chem. Rev.* **1967**, *2*, 3.
(20) Gutman, I.; Trinajstić, N. *Top. Curr. Chem.* **1973**, *42*, 49.
(21) Biggs, N. L. *Algebraic Graph Theory*; Cambridge University Press: London, 1974; p 9.
(22) King, R. B.; Rouvray, D. H. *J. Am. Chem. Soc.* **1977**, *99*, 7834.
(23) King, R. B. In *Chemical Applications of Topology and Graph Theory*; King, R. B., Ed.; Elsevier: Amsterdam, 1983; pp 99-123.
(24) King, R. B. In *Molecular Structure and Energetics*; Liebman, J. F., Greenberg, A., Eds.; VCH: Deerfield Beach, FL, 1976; pp 123-148.
(25) King, R. B. *Rep. Mol. Theor.* **1990**, *1*, 141.
(26) Wilson, R. J. *Introduction to Graph Theory*; Oliver and Boyd: Edinburgh, 1972; p 16.
(27) King, R. B. *J. Comput. Chem.* **1987**, *8*, 341.
(28) Hoffmann, R.; Lipscomb, W. N. *J. Chem. Phys.* **1962**, *36*, 2179.
(29) Pope, M. T. *Heteropoly and Isopoly Oxometallates*; Springer-Verlag: Berlin, 1983.
(30) Day, V. W.; Klemperer, W. G. *Science* **1985**, *228*, 533.
(31) Launay, J. P.; Babonneau, F. *Chem. Phys.* **1982**, *67*, 295.
(32) Cairns, C. J.; Busch, D. H. *Coord. Chem. Rev.* **1986**, *69*, 1.
(33) Ref 21, p 14.
(34) Prados, R. A.; Pope, M. T. *Inorg. Chem.* **1976**, *15*, 2547.
(35) Varga, G. M., Jr.; Papaconstantinou, E.; Pope, M. T. *Inorg. Chem.* **1970**, *9*, 662.
(36) Robin, M. B.; Day, P. *Adv. Inorg. Chem. Radiochem.* **1967**, *10*, 247.
(37) Lennay, J. P.; Fournier, M.; Sanchez, C.; Livage, J.; Pope, M. T. *Inorg. Nucl. Chem. Lett.* **1980**, *16*, 257.
(38) Barrows, J. N.; Pope, M. T. *Adv. Chem. Ser.* **1990**, *226*, 403.

Combinatorics of Cluster Enumeration

K. BALASUBRAMANIAN†

Department of Chemistry, Arizona State University, Tempe, Arizona 85287-1604

Received August 27, 1991

Recent developments in the enumeration of isomers of gallium arsenide clusters of the formula Ga_xAs_y as well as hydrogenated clusters of C_{60} such as $C_{60}H_n$ and deuterated clusters $C_{60}H_nD_m$ are reviewed. The procedures for the combinatorical enumeration of isomers of $C_{60}H_nX_m$ are also outlined. The nuclear spin statistics and the classification of rotational levels of $C_{60}H_{60}$ and $C_{60}D_{60}$ are considered using combinatorical methods.

1. INTRODUCTION

Clusters have been the topic of an increasing number of theoretical and experimental studies in recent years.[1-23] The increased interest stems from several experimental studies. The first and also the most important investigation from the standpoint of impact is the synthesis and characterization of the "buckminsterfullerene" or the C_{60} clusters.[6-8] The aesthetically appealing soccerball-shaped cluster generated intense experimental and theoretical activity on the topic. The theoretical studies included numerous semiempirical and ab initio studies as well as topological characterization of related clusters. The C_{60} cluster also revived the resonance theory of polycyclic molecules containing carbon atoms. The C_{60} cluster also generated topological interest on other forms of platonic solids.

The recent synthesis of gram quantities of C_{60} as well as $C_{60}H_{36}$, $C_{60}H_{60}$, and other molecules[21] generated by the Birch reduction has provided significant impetus for the ab initio and graph theoretical studies for the hydrogenated C_{60} cluster.

Another interesting set of clusters of great importance in the semiconductor area is the cluster of gallium arsenide of the general formula, Ga_xAs_y. O'Brien et al.[1] produced these clusters using the laser vaporization of pure GaAs crystal. A fascinating finding of O'Brien et al. is that the smaller clusters deviated significantly from the binomial distribution of relative abundance while the large clusters followed a binomial distribution. It is not evident whether the strong deviation displayed by the smaller clusters is due to inherent extra stability (magic numbers) or if this is due to the possibility of greater number of isomers (long-lived) with that particular molecular formula.

Ab initio cluster computations also require often-possible structures for a given cluster. Codes which do not have automated geometry optimization techniques especially require as input possible geometries for energetics consideration.

The experimentally observed fragmentation patterns for clusters are also very intriguing. The explanation of the

† Camille and Henry Dreyfus Teacher-Scholar.

0095-2338/92/1632-0047$03.00/0